Development 140, 770-779 (2013) doi:10.1242/dev.088898

ZHOUPI controls embryonic cuticle formation via a signalling pathway involving the subtilisin protease ABNORMAL LEAF-SHAPE1 and the receptor kinases GASSHO1 and GASSHO2

Qian Xing[1], Audrey Creff[2], Andrew Waters[1], Hirokazu Tanaka[3], Justin Goodrich[1] and Gwyneth C. Ingram[2,*]

SUMMARY

Seed production in angiosperms requires tight coordination of the development of the embryo and the endosperm. The endosperm-specific transcription factor ZHOUPI has previously been shown to play a key role in this process, by regulating both endosperm breakdown and the formation of the embryonic cuticle. To what extent these processes are functionally linked is, however, unclear. In order to address this issue we have concentrated on the subtilisin-like serine protease encoding gene *ABNORMAL LEAF-SHAPE1*. Expression of *ABNORMAL LEAF-SHAPE1* is endosperm specific, and dramatically decreased in *zhoupi* mutants. We show that, although *ABNORMAL LEAF-SHAPE1* is required for normal embryonic cuticle formation, it plays no role in regulating endosperm breakdown. Furthermore, we show that re-introducing *ABNORMAL LEAF-SHAPE1* expression in the endosperm of *zhoupi* mutants partially rescues embryonic cuticle formation without rescuing their persistent endosperm phenotype. Thus, we conclude that ALE1 can normalize cuticle formation in the absence of endosperm breakdown, and that *ZHOUPI* thus controls two genetically separable developmental processes. Finally, our genetic study shows that ZHOUPI and ABNORMAL LEAF-SHAPE1 promotes formation of embryonic cuticle via a pathway involving embryonically expressed receptor kinases GASSHO1 and GASSHO2. We therefore provide a molecular framework of inter-tissue communication for embryo-specific cuticle formation during embryogenesis.

KEY WORDS: Cell death, cuticle, Embryo, Endosperm, Seed development, Signalling

INTRODUCTION

Seed production in angiosperms requires a tight coordination of the development of the two zygotic products of double fertilization: the embryo and the endosperm. In the model species *Arabidopsis thaliana*, the endosperm is a largely transitory structure, which has been shown to play an important role in driving the expansion of the maternally derived seed coat early in seed development (Garcia et al., 2003), but which then breaks down, permitting the developing embryo to fill the seed at later stages. At maturity, only a single-cell layer of endosperm tissue remains surrounding the dormant embryo (Bethke et al., 2007; Penfield et al., 2004). The importance of the coordination of endosperm breakdown with embryo growth is exemplified in basic helix-loop-helix transcription factor ZHOUPI loss-of-function mutants, in which endosperm breakdown does not occur, leading to the production of a persistent endosperm and an embryo of drastically reduced size (Kondou et al., 2008; Yang et al., 2008).

ZOU is expressed exclusively in endosperm cells surrounding the developing embryo, and it is therefore likely that its role in driving endosperm breakdown is cell-autonomous (Yang et al., 2008). Interestingly however, the phenotype of *zou* mutants is not restricted to endosperm persistence and decrease in embryo size. A second embryonic phenotype, consisting of cuticle abnormalities and an extreme desiccation intolerance upon germination, has also been described (Kondou et al., 2008; Yang et al., 2008). Consistent with cuticular abnormalities, the embryos of *zou* mutants adhere tightly to surrounding endosperm tissues both during development and upon germination, when the remains of the persistent endosperm can be observed on the cotyledon surface (Yang et al., 2008). Despite these severe seed and seedling phenotypes, *zou* mutant seeds germinate and give rise to phenotypically normal homozygous plants, if seedlings are maintained in a humid environment during their early development.

The epidermal phenotype of *zou* mutants is intriguing, as cuticle biogenesis is widely understood to be an epidermal property and thus to be mediated by the epidermal cells of the developing embryo. Two possible, and not necessarily mutually exclusive, explanations could account for the cuticular defects in *zou* mutants. First, the close proximity of the abnormally persistent endosperm in *zou* mutants could make it difficult for the epidermal cuticle of the embryo to mature correctly, and lead to a boundary 'blurring' between the two structures. Alternatively, ZOU could regulate embryonic cuticle formation independently of endosperm breakdown, via a non-cell-autonomous pathway.

In terms of cuticle formation, the angiosperm embryo is unique, as all other cuticle-bearing surfaces in the aerial part of the plant are juxtaposed either by the atmosphere, or by other epidermally derived cuticle-bearing surfaces on adjacent organs. The cuticularization of juxtaposed surfaces has been shown to be extremely important for the definition of organ boundaries, both during development and postgenitally. Mutants with compromised cuticles often show extensive organ fusions (Kurdyukov et al., 2006a; Kurdyukov et al., 2006b; Lolle et al., 1992; Pruitt et al., 2000; Wellesen et al., 2001; Yephremov et al., 1999). Several genetic lesions that affect cuticle biogenesis either exclusively, or predominantly, in the developing embryo have been described,

[1]Institute of Molecular Plant Sciences, University of Edinburgh, King's Buildings, Mayfield Road, Edinburgh EH9 3JH, UK. [2]Laboratoire Reproduction et Développement des Plantes, UMR 5667 CNRS-INRA-ENS-Lyon-UCB Lyon I, IFR 128 BioSciences Gerland-Lyon Sud, ENS Lyon, 46 Allée d'Italie, 69364 LYON Cedex 07, France. [3]Laboratory of Plant Growth and Development, Department of Biological Science, Graduate School of Science, Osaka University, 1-1 Machikaneyama-cho, Toyonaka-shi, Osaka 560-0043, Japan.

*Author for correspondence (gwyneth.ingram@ens-lyon.fr)

Accepted 30 November 2012

consistent with the hypothesis that the unique situation of the embryo requires the activity of specific developmental pathways for the production of a functional cuticle. These lesions include the simultaneous loss of two related and functionally redundant receptor-like kinase-encoding genes, *GASSHO1* and *GASSHO2* (*GSO1* and *GSO2*) (Tsuwamoto et al., 2008), and mutations in a gene encoding a Subtilisin-like Serine protease, ABNORMAL LEAF SHAPE1 (ALE1) (Tanaka et al., 2001; Tanaka et al., 2004). Although GSO1 and GSO2 are expressed in the embryo, the expression of ALE1 is restricted to the endosperm surrounding the embryo (Tanaka et al., 2001). An extracellular localization for ALE1 protein has been predicted, leading to speculation that endosperm-derived information could be important for normal embryonic cuticle formation (Rautengarten et al., 2005).

The expression patterns of *ZOU* and *ALE1* are strikingly similar, and we have previously shown that the transcription of *ALE1* is strongly reduced in *zou* mutants and that *ZOU* is epistatic to *ALE1*, consistent with both genes acting in the same developmental pathway (Yang et al., 2008). The cuticle phenotype of *ale1* mutants is reminiscent of, although milder than, that of *zou* mutants. However, despite the fact that the endosperm tissues have been reported to adhere to the surface of *ale1* mutant embryos during their development (Tanaka et al., 2001), it has so far been unclear whether an endosperm breakdown defect is associated with loss of *ALE1* function. Two scenarios can be envisaged: (1) *ALE1* acts downstream of *ZOU* in a pathway regulating both endosperm breakdown and cuticle formation; (2) *ZOU* regulates two developmental processes – endosperm breakdown (via an *ALE1* independent pathway) and embryo cuticle formation via a non-cell-autonomous pathway involving *ALE1*. In order to distinguish between these hypotheses, we have analysed whether *ALE1* plays a role in regulating endosperm cell death, and investigated whether the cell death regulation and cuticle formation functions of ZOU can be separated during seed development. We have also studied the genetic relationship between the endosperm-specific genes *ALE1* and *ZOU*, and the genes encoding the embryonically expressed receptors *GSO1* and *GSO1*, to elucidate their potential roles in signalling between the endosperm and the embryo.

MATERIALS AND METHODS

Plant materials and growth conditions

Mutant lines used in this study have been published previously with the exception of *ale1-3* (SAIL_736_D09/N862715) and *ale1-4* (SAIL_279_C04/N812918). General plant culture conditions were long (16 hour) days at 21°C. For staged material for phenotypic and transcriptional analysis, plants were grown at 16°C in continuous light. These conditions give a uniform slow rate of flower emergence and silique development, allowing more accurate staging of embryonic development. Tissue culture (for Toluidine Blue staining) was carried out in a Lemnagen growth cabinet under long (16 hour) days at 21°C.

Seed clearing

To visualize and stage developing seeds, siliques were opened with needles, and the seeds were removed with forceps into a drop of clearing solution (8 g chloral hydrate, 2 ml water, 1 ml glycerol). Coverslips were applied and samples were incubated at 4°C overnight before visualization under DIC optics using a Zeiss AX10.

Toluidine Blue staining

Seeds were spread uniformly on 15 cm plates containing 1×MS Basal Salts (Duchefa), 0.3% sucrose and 0.4% Phytagel (Sigma) (pH 5.8). Stratification was carried out at 4°C for 3 days before transferring plates to a growth room for 7 days. Lids were removed and plates were immediately flooded with staining solution [0.05% (w/v) Toluidine Blue + 0.4% (v/v) Tween-20] for 2 minutes. The staining solution was poured off and plates were immediately rinsed gently by flooding under a running tap until the water stream was no longer visibly blue (1-2 minutes). Seedlings were photographed, or harvested for Toluidine Blue quantification. To harvest, seedlings were removed individually from plates and both roots and any adhering seed coats (both of which stain darkly with Toluidine Blue) were completely removed before plunging the hypocotyl and cotyledons into 1 ml of 80% ethanol. Seedlings were incubated with continuous shaking for 2 hours, until all blue colour and chlorophyll had been removed from cotyledons. The resulting liquid was analyzed using a spectrophotometer.

Test for seedling desiccation tolerance

Batches of 100 seeds were counted, plated on MS-Agar (0.5% Sucrose), stratified at 4°C for 3 days, and allowed to germinate in the standard growth chamber conditions for 7 days. All resulting seedlings were transferred to small pots containing moist compost in mixed trays, and covered with a loosely fitted lid for 3 days to allow root establishment. Pots were arranged in a random block design in trays, ensuring an equal exposure to potential border effects for each genotype. Moreover, trays were rotated once daily in order to minimise any heterogeneity owing to shelf position. The lid was then completely removed. Trays were kept uniformly moist, and seedling survival was counted after a period of 3 weeks.

Resin embedding and sectioning

Mature seeds were removed from siliques and vacuum infiltrated at 4°C with 4% paraformaldehyde + 5% glutaraldehyde in PBS (pH 7) with 1% Triton-X-100 (Sigma), 0.1% TWEEN (United States Biological) and 1% DMSO. Samples were incubated at 4°C overnight with continuous shaking, rinsed thoroughly with ice-cold PBS and dehydrated through a cold ethanol series into dry ethanol. Ethanol was then substituted sequentially for LR-White Hard Grade resin over 4-5 days. Samples were incubated in several changes of 100% resin over at least 3 days before placing individual seeds into size 00, snap-fit, gelatine capsules (Agar Scientific, G3740). Resin was polymerized for 24 hours at 60°C. Sections (1 μm) were cut using glass knives on an ultramicrotome, and dried onto glass slides where they were stained for 10 seconds at 70°C with filtered 1% Toluidine Blue/1% borax before rinsing with distilled water, drying and mounting in Eukitt mounting medium (Fluka). Alternatively, fixed, dehydrated samples were embedded in Technovit 7100 resin following the manufacturer's instructions (Heraeus Kulzer GmbH). Sections (1.5 μm) were cut using a metal knife on a Zeiss Hm355 S microtome, floated onto glass slides, dried, oxidized for 10 minutes in 1% periodic acid, washed for 5 minutes under running tap water, stained for 5 minutes in Schiff's reagent (Sigma-Aldrich), washed for 5 minutes, dried and mounted as above.

Quantitative gene expression analysis

In order to obtain staged material, all plants were grown under near identical conditions. Every silique on the main inflorescence spike of selected individuals of each genotype was dissected and cleared in order to ascertain the synchronicity of the population. Pools of siliques were then harvested from the remaining individuals in such a way that each sample contained one discrete developmental stage. A single biological replicate contains three or four siliques from one individual plant. Total RNA was extracted using the Spectrum Plant Total RNA Kit (Sigma). Total RNAs were digested with Turbo DNA-free DNase I (Ambion) according to the manufacturer's instructions. RNA concentration and integrity were measured after DNase I digestion with a NanoDrop ND-1000 UV-Vis spectrophotometer (NanoDrop Technologies). RNA (1 μg) was reverse transcribed using the SuperScript VILO cDNA Synthesis Kit (Invitrogen) according to the manufacturer's protocol. PCR reactions were performed in an optical 96-well plate in the StepOne Plus Real Time PCR System (Applied Biosystems), using Platinum SYBR Green qPCR SuperMix-UDG in a final volume of 20 μl, according to the manufacturer's instructions. The following standard thermal profile was used for all PCR reactions: 50°C for 2 minutes, 95°C for 2 minutes, 40 cycles of 95°C for 15 seconds, 60°C for 20 seconds and 72°C for 20 seconds. Amplicon dissociation curves, i.e. melting curves, were recorded after cycle 40 by heating from 60°C to 95°C with a ramp speed of 1°C/minute. Data were analyzed using the StepOne Software v2.2

(Applied Biosystems). As a reference, primers for the EIF4A cDNA were used (all primers used in Q-PCR analysis are listed in supplementary material Table S1). PCR efficiency (E) was estimated from the data obtained from standard curve amplification using the equation $E=10^{-1/\text{slope}}$. The expression level of each gene of interest (GOI) is presented as $E^{-\Delta Ct}$, where $\Delta Ct=Ct_{GOI}-Ct_{EIF4A}$.

Generation of whole-transcriptome sequence data

Single-run whole transcriptomes were generated for staged siliques from individual *zou-4*, *ale1-4* and Col0 plants at the early heart and early torpedo stage. Plants were grown under identical conditions. In each case, five independent RNA samples were extracted (as above) for each genotype, quality was ascertained using an Agilent Bioanalyser and the three highest quality samples were pooled. Sequencing of the six resulting samples was carried out on an Illumina HiSeq 2000 by GATC Biotech. Twelve- to 14-million reads were generated for each sample, and subjected to quality control and mapped onto gene models (TAIR 10 release) using in-house (GATC) software, and normalized to reads per kilobase per million (RPKM). We considered genes to be significantly expressed at a given stage if RPKM values were above 5 (corresponding to at least 60 reads for a 1 kb gene in our data) in the relevant Col0 sample. Genes selected for further analysis showed a greater than halving in RPKM value in *ale1-4* and/or *zou-4* samples at both the early heart and the early torpedo stage. Full datasets are available on request.

Genotyping

Plant DNA was extracted with a rapid CTAB isolation technique as described by Stewart and Via (Stewart and Via, 1993). The pellet was air dried, resuspended in 100 µl of TE and RNase A treated for 30 minute at 37°C. DNA (1 µl) was used to perform PCR reactions. Genotyping for *zou4* and *ale1-1* was carried out as previously described (Tanaka et al., 2001; Yang et al., 2008). Genotyping of *ale1-4* was carried out using the primers geno-ale1-4-R (TGTAGTTCACAATCTTATCAATCTGG) and genoALE1 (TGTAGTTCACAATCTTATCAATCTGG). Genotyping of *ale1-3* was carried out using primers ALE1-F (AGGGCGTTGGACTATCAGG), ALE1cDNAR (CAATAAAATTTTATGTTTTCAAATGG) and LB3 (TAGCATCTGAATTTCATAACCAATCTCGATACAC). Genotyping of *gso-1* and *gso2-1* mutant alleles was carried out exactly as described previously (Tsuwamoto et al., 2008).

RESULTS

The ZOU target gene *ALE1* is involved in embryonic cuticle formation but not endosperm autolysis

The expression of *ALE1* is dramatically downregulated in *zou* mutant backgrounds (Yang et al., 2008). As *ALE1* is the only *ZOU*-regulated gene for which mutants share elements of the zou phenotype (namely cuticle defects in cotyledon tissues), we decided to further explore the function of *ALE1* in seed development, and in particular whether it plays any role in regulating endosperm breakdown. The first published mutant alleles of *ALE1*, *ale1-1* and *ale1-2,* were isolated in the Landsberg *erecta* (L*er*) background (Tanaka et al., 2001). *ale1-1* was subsequently introgressed into the Columbia-0 (Col0) background by successive backcrossing. In order to confirm that the phenotype of this line corresponds to that of *ale1* loss of function in a pure Col-0 background, we also characterized two new T-DNA insertion alleles of *ALE1,* which we have named *ale1-3* and *ale1-4*. *ale1-3* contains a T-DNA insertion in the last intron of *ALE1*, whereas in *ale1-4*, a T-DNA is inserted just upstream of the start of transcription, where it would be expected to interfere with regulatory sequences (Fig. 1A). Q-RT-PCR analysis of *ALE1* transcripts in cDNA from young siliques of wild-type plants showed strong expression of *ALE1* from the globular stage onwards. Although *ale1-1* siliques expressed transcripts at low levels (supplementary material Fig. S1), *ale1-3* and *ale1-4* siliques were found to express no detectable *ALE1* transcripts at mid-seed development (supplementary material Figs S1, S2) and thus represent true null alleles of *ALE1*.

Consistent with transcriptional analysis, *ale1-1*, *ale1-3* and *ale1-4* homozygous seedlings showed patches of staining on cotyledons when treated with Toluidine Blue, suggesting that they show similar cuticle defects (Fig. 1D,E; supplementary material Fig. S3) (Tanaka et al., 2004). These patches tended to be larger in *ale1-3* and *ale1-4* than in *ale1-1*, and were generally smaller than those previously seen for *ale1-1* in the L*er* background. As previously

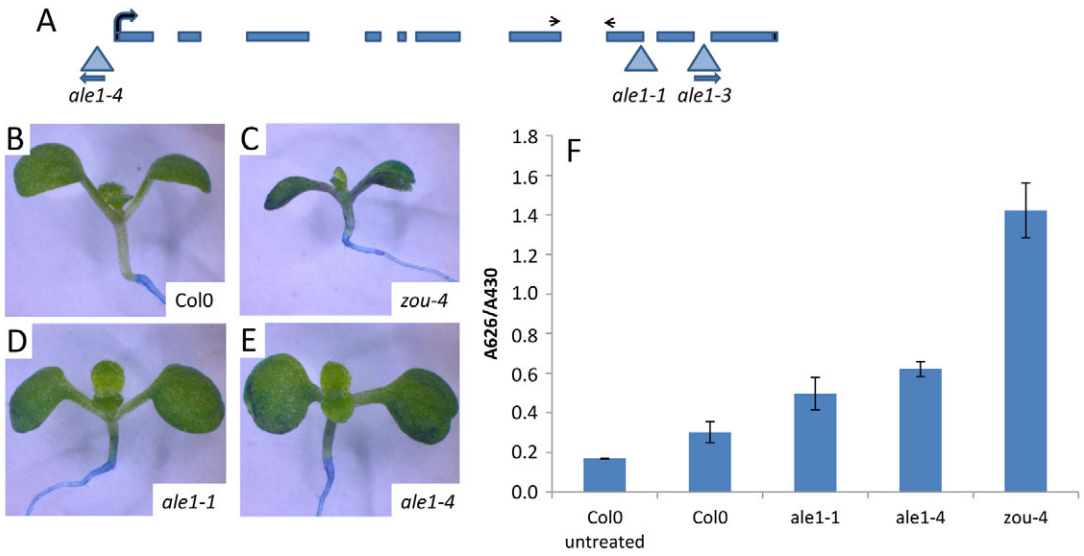

Fig. 1. Loss of *ALE1* function in a Col0 background causes weak seedling cuticle defects. (**A**) The *ALE1* gene. Exons are represented as blue boxes. The transcription start is shown as a thick black arrow. Positions of primers used in Q-PCR analyses are shown as small black arrows. Positions of T-DNA and transposon insertions in mutant alleles are shown as blue triangles, with the orientation of the T-DNA left borders indicated. (**B-E**) Toluidine Blue staining of wild-type (B), *zou-4* (C), *ale1-1* (D) and *ale1-4* (E) mutant seedlings 7 days after germination. All seedlings were grown on the same plate in order to permit uniform processing. (**F**) Toluidine Blue uptake in these lines was quantified spectrophotometrically, showing the weak cotyledon cuticle phenotypes of *ALE1* alleles compared with *zou* mutant seedlings. Error bars represent s.d. between three biological replicates each containing 20 seedlings.

reported, *zou-4* seedlings showed a strong staining with Toluidine Blue, consistent with severely compromised cuticle function (Fig. 1C; supplementary material Fig. S3) (Yang et al., 2008). Wild-type seedlings showed no visible permeability to Toluidine Blue stain (Fig. 1B; supplementary material Fig. S3). In order to further investigate this phenotype, we developed a method of quantifying Toluidine Blue uptake by seedlings grown *in vitro*, and stained for a defined period of time (see Materials and methods). Briefly, Toluidine Blue enters cotyledons via the defective cuticle and binds strongly to cell walls within the organ (Tanaka et al., 2004). Washing to remove excess external Toluidine Blue has little effect on internalized stain. Internalized stain can, however, be solubilized in 80% ethanol and quantified spectroscopically (Terry et al., 2000). This method proved robust, and allowed us to measure Toluidine Blue uptake relative to cotyledon volume (approximated by Abs 430, an absorbance peak for Chlorophyll A, see supplementary material Fig. S10 for details). Although we could easily distinguish Col0, *ale1* mutants and *zou-4* using this method, we were not able to show a statistically significant difference in cuticle defects between *ale1-1*, *ale1-3* and *ale1-4* (Fig. 1F; supplementary material Fig. S3).

Seed morphology was studied for all three alleles, and revealed a previously undescribed aspect of the ale1 phenotype: a significant rate of formation of visibly mis-shapen seeds. Again, the frequency of misshapen seeds was higher in the *ale1-4* background (74%) than in the *ale1-1* background (47%). The abnormal seed phenotype is typically characterised by 'lumpy' seeds, which tend to be rounder than wild-type seeds, which are smoother and more elliptical (Fig. 2). In order to follow embryo development more closely, seeds were cleared and observed using DIC microscopy. Early embryo development in *ale1-4* mutants and *zou-4* was indistinguishable from that in the wild-type background (Fig. 3A,E,I). However, by the walking stick stage (Fig. 3D,H,L), mis-oriented embryo growth was observed at a frequency of 72% (n=150) in *ale1-4* mutants (Fig. 3L) and 28% (n=170) in *ale1-1* mutants. By this stage, embryo growth in *zou-4* mutants (Fig. 3H) was severely retarded, and the persistent endosperm that characterizes *zou* mutants was evident. Although slight growth retardation was observed for adherent *ale1-4* embryos, no significant endosperm persistence was noted in any of the *ale1* alleles studied.

To further investigate endosperm persistence at seed maturity, mature green (non dessicated) seeds were fixed, resin embedded and sectioned. Wild-type seeds at this stage contain a single layer of specialized endosperm cells, which are maintained throughout, and necessary for, seed dormancy (Bethke et al., 2007) (Fig. 3M). In *zou-4* mutants, a significant body of endosperm tissue persists at seed maturity (Fig. 3N; supplementary material Fig. S8), shrivelling upon desiccation to give *zou* seeds their distinctive appearance. Resin sections revealed that the specialized outer endosperm-cell monolayer seen in wild type is still differentiated normally in *zou* mutants, whereas the remaining persistent endosperm is composed of large, highly vacuolated cells with thin walls (Fig. 3N; supplementary material Fig. S8). In both *ale1-1* and *ale1-4* mutant backgrounds, only a single layer of endosperm cells was observed (Fig. 3O), similar to the situation in wild-type plants. Consistent with this observation, no seed shrivelling was apparent in any of the *ale1* mutant backgrounds studied.

The expression of a subset of genes misegulated in *zou* mutants, is also affected in *ale1* mutants

In order to understand more about the molecular basis for the defects presented by *zou* and *ale1* mutants, a transcriptomic analysis of siliques containing embryos at the late heart/early torpedo stage of development from *zou-4*, *ale1-4* and Col0 plants was performed (see Materials and methods). Genes showing significant downregulation in *zou* mutant background fell into two classes: those whose expression was also significantly downregulated in *ale1-4* (including the *ALE1* gene), and those in

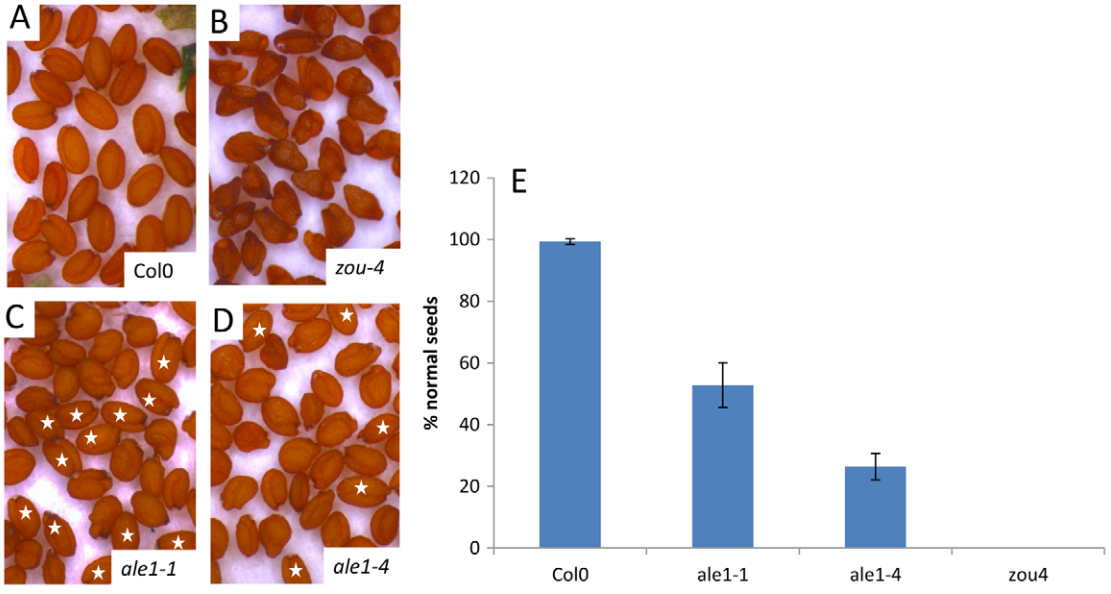

Fig. 2. ALE1 function is required for normal seed shape. (**A-D**) Seed phenotypes of Col0 (wild type) (A), *zou-4* (B), *ale1-1*(C) and *ale1-4* (D). In all cases, seeds were obtained from homozygous mutant lines. (B,E) All seeds of *zou-4* mutants are abnormal and show the published shrivelled seed phenotype. (C,E) In *ale1-1*, ~50% of seeds are indistinguishable from those of wild-type plants (stars), with the remainder showing defects in seed shape. (D,E) In *ale1-4*, the percentage of normal-looking seeds drops to around 25% (stars), and some mis-shapen seeds appear smaller than those of wild-type plants. (**E**) Seed shape counts were carried out on biological triplicates (100 seeds per plant from three homozygous individual). Error bars represent s.d. between biological triplicates.

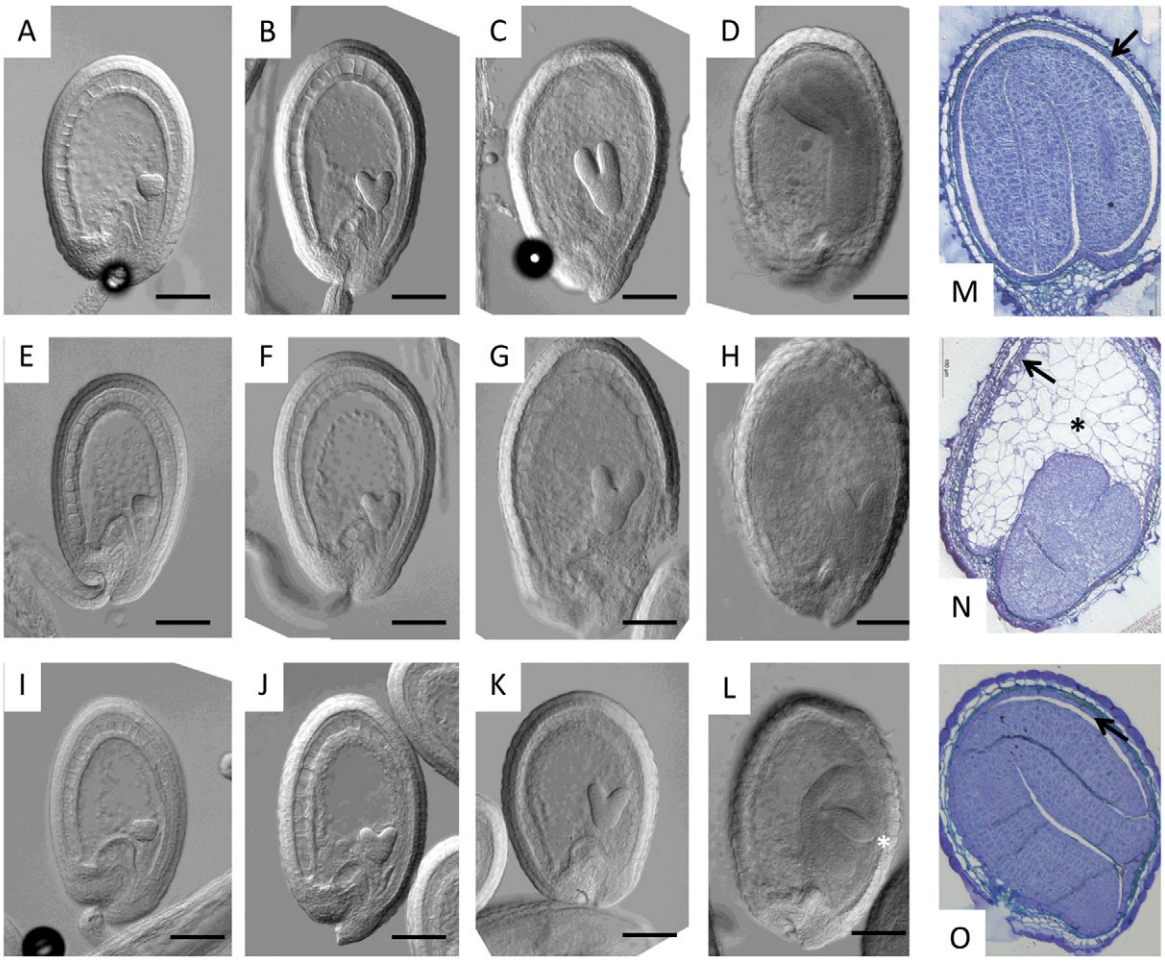

Fig. 3. Loss of *ALE1* function causes adhesion to the endosperm, but no endosperm persistence. (**A-L**) Cleared seeds from Col0 (A-D), *zou-4* (E-H) and *ale1-4* (I-L) at late globular (A,E,I), mid-heart (B,F,J), late heart (C,G,K) and walking stick (D,H,L) stages of embryo development. Adhesion of the cotyledon of an *ale1-4* seedling to the surrounding endosperm tissue is shown by an asterisk in L. (**M-O**) Resin-embedded and sectioned mature, non-desiccated seeds from Col0 (M), *zou-4* (N) and *ale1-1* (O). The persistent endosperm in *zou-4* is indicated by an asterisk in N. The 'aleurone-like' cell layer is indicated by arrows (M-O). Scale bars: 50 μm.

whose expression levels in *ale1* mutants were indistinguishable from those in wild type [including four of the six published ZOU targets previously identified by microarray analysis (Kondou et al., 2008)]. Confirmation of mis-regulation was carried out for a subset of genes predicted to be expressed in the endosperm and/or embryo based on *in silico* data (Le et al., 2010), using Q-PCR in developing siliques of *zou-4*, *ale1-4* and Col0 plants grown under identical conditions. Data for three genes regulated specifically by ZOU, and two genes regulated both by ZOU and ALE1 are shown in supplementary material Fig. S4. These results support our phenotypic and genetic data showing that *ZOU* and *ALE1* perform partially, but not totally, overlapping functions.

ALE1 expressed under the SUC5 promoter rescues ale1 seed and cotyledon phenotypes

Our results support a model in which *ZOU* regulates both cell breakdown in the endosperm and embryonic cuticle formation, whereas *ALE1* is uniquely required for embryonic cuticle development. To investigate whether the two proposed functions of ZOU can be separated, a construct was generated that would permit the expression of *ALE1* in a *ZOU*-independent fashion. Previous work from our laboratory had identified expression of the gene *AtSUC5* (Baud et al., 2005), as being independent of *ZOU* activity (Yang et al., 2008). The published expression pattern of *AtSUC5* is very similar to that of *ZOU* and *ALE1*, in that it is largely restricted to the endosperm surrounding the developing embryo during seed development (Baud et al., 2005). We therefore made a construct to express the *ALE1* open reading frame under the control of the *AtSUC5* promoter (*pSUC5::ALE1*), and thus render *ALE1* expression independent of *ZOU* activity.

To confirm the ability of this construct to recapitulate wild-type *ALE1* expression and function, homozygous transformants in a Col0 background were crossed into the *ale1-1* mutant background and F2 plants homozygous for both *ale1-1* and the *pSUC5::ALE1* transgene were selected for further analysis. The phenotypes of resulting plants were assessed both for cotyledon cuticle defects and for seed morphology, and showed a complete complementation of both phenotypes (supplementary material Fig. S5).

Expression of ALE1 under the pSUC5 promoter complements zou cuticle defects, but does not restore endosperm autolysis

The *pSUC5::ALE1* construct was introduced into a *zou-4* mutant background. Transformed lines were screened for *ALE1* expression

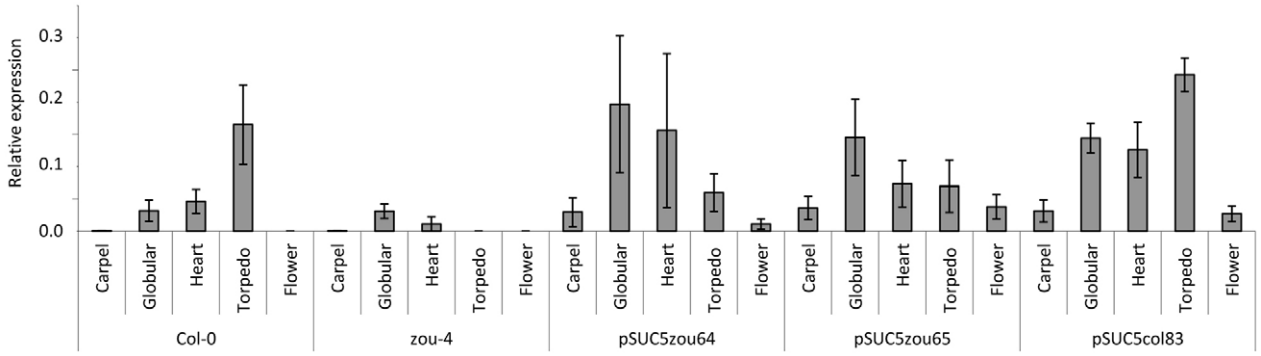

Fig. 4. Expression of *ALE1* relative to that of *EIF4* in Col0, *zou-4, zou-4[pSUC5::ALE1]-8, zou-4[pSUC5::ALE1]-26* and Col0*[pSUC5::ALE1]-10* backgrounds. Staging of embryos is shown in supplementary material Fig. S6. Results are from biological triplicates, each of which was analysed in technical triplicate. Error bars represent s.d. between biological triplicates.

level by Q-PCR. Two lines with increased expression of *ALE1* in a *zou-4* background (line 8 and line 26) and one in a wild-type background were selected for further analysis. The expression of *ALE1* in these lines was compared in detail with its expression in *zou-4* mutants and in wild-type plants by collecting staged tissue samples corresponding to five developmental stages: inflorescence tips containing unopened flowers (flower), siliques containing preglobular stage embryos, siliques containing seeds with mid globular-stage embryos, siliques containing seeds with mid heart-stage embryos and siliques containing seeds with early torpedo stage embryos (see supplementary material Fig. S6 for staging). In wild-type tissues, the expression of endogenous *ALE1* initiated at the globular stage and became increasingly strong at subsequent developmental stages (Fig. 4). Expression of *ALE1* in *zou-4* mutants was similar to wild type at the globular stage, but was then not maintained and fell back to very low levels at older stages. Expression of *ALE1* in *zou-4* plants transformed with *pSUC5:ALE1* was considerably stronger than in either *zou-4* or wild-type tissues at the globular stage, and then fell back to levels higher than those in *zou-4* mutants, but lower than those in wild type at later stages. Wild-type plants containing *pSUC5:ALE1* showed an *ALE1* expression pattern that was effectively additive between wild type and transgene expression (Fig. 4). A basal level of *ALE1* expression was also observed in inflorescence samples from all plants transformed with *pSUC5:ALE1*, suggesting that, as previously shown, *pSUC5*-driven expression is not entirely seed specific (Baud et al., 2005). It therefore appears that the pattern of expression of *SUC5* during seed development is spatially similar, but temporally not identical to that of *ALE1*.

In order to ascertain the phenotypic effects of restoring *ALE1* expression in a *zou* background, the *zou-4* lines transformed with *pSUC5:ALE1* were compared with *zou-4* and wild type at the level of seed and seedling morphology, Toluidine Blue staining and seedling desiccation tolerance. At the level of seed morphology, both lines were indistinguishable from *zou-4,* in that they produced small, dark wrinkled seeds with an obvious ‘pouch’ of persistent endosperm surrounding a small embryo (Fig. 5E,F). Clearing of developing seeds from both transgenic lines and *zou-4* revealed no visible difference in the amount of persistent endosperm observed at any developmental stage, although the ‘cavity’ surrounding the embryo was more often apparent in the transformed lines than in *zou-4* (Fig. 5C,D). No phenotypic effects of overexpressing ALE1 in a wild-type background were observed. From these data, we conclude that no significant diminution in endosperm persistence is caused by the transcription of *ALE1* in *zou-4* mutants. This conclusion was confirmed by resin sectioning of seeds from the *zou-4* line, showing the strongest level of *ALE1* expression under the *AtSUC5* promoter (line 8). The endosperm persistence in this line is indistinguishable from that in an untransformed *zou-4* mutant (supplementary material Fig. S7).

When seeds were imbibed and dissected, it was considerably easier to separate the embryo and endosperm tissues of the *zou-4*

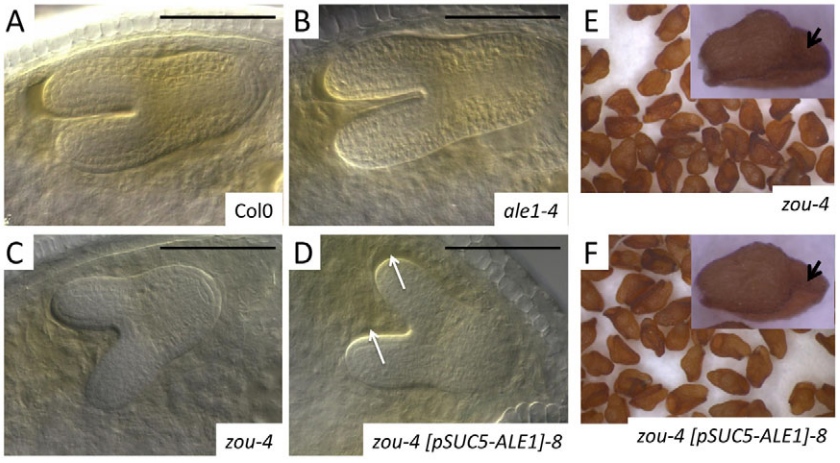

Fig. 5. Reintroducing *ALE1* expression into a *zou-4* background partially rescues endosperm adhesion defects but does not rescue seed shrivelling. (**A-D**) Cleared embryos in seeds from Col0 (A), *ale1-4* (B), *zou-4* (C) and *zou-4[pSUC5::ALE1]-8* (D) taken at the early torpedo stage in development. The growth defect in *zou-4* mutants is evident at this stage. No obvious difference in embryo development is seen between *zou-4* and *zou-4[pSUC5::ALE1]-8,* but separation between the embryo and endosperm (arrows) is observed in *zou-4[pSUC5::ALE1]-8.* (**E**,**F**) Seeds from *zou-4* (E) and *zou-4[pSUC5::ALE1]-8* (F) plants look identical. Arrows in E and F indicate the pouch of persistent endosperm present in *zou* seeds. Scale bars: 50 μm.

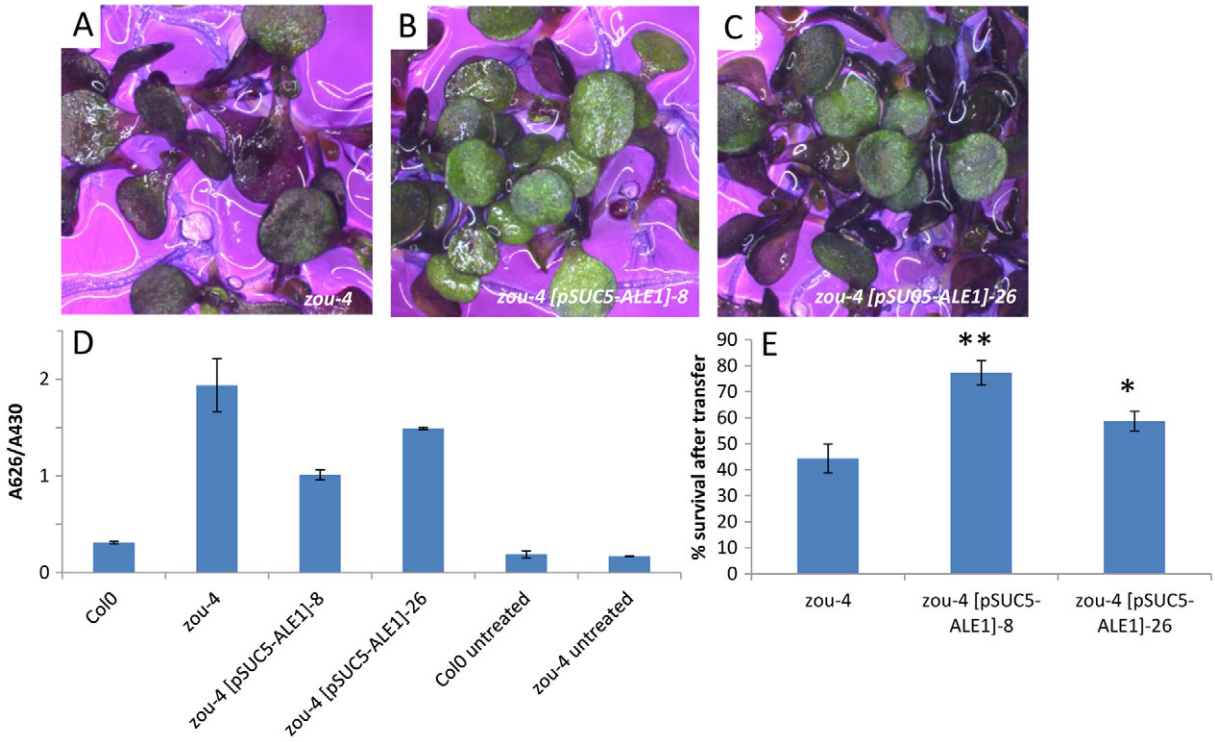

Fig. 6. Re-introducing *ALE1* expression into a *zou-4* background partially rescues seedling cuticle defects and seedling resistance to desiccation. (**A-C**) Toluidine Blue staining of *zou-4* (A), *zou-4[pSUC5::ALE1]-8* (B) and *zou-4[pSUC5::ALE1]-26* (C) seedlings 7 days after germination. All seedlings were grown on the same plate in order to permit uniform processing. (**D**) Toluidine Blue uptake in these lines was quantified spectrophotometrically (D), showing a significant rescue of the *zou-4* cuticle phenotype, particularly in *zou-4[pSUC5::ALE1]-8*. Error bars represent s.d. between three biological replicates each containing 20 seedlings. (**E**) Seedling desiccation tolerance was tested on three independent samples of 100 seeds grown in homogenized conditions. Error bars represent the s.d. between biological replicates. **P*<0.05, ***P*<0.01 compared with *zou-4* in pairwise tests (Tukey's HSD). ANOVA shows significant differences between all three samples (*P*<0.01).

lines transformed with pSUC5::ALE1, than of *zou-4* mutant seed. It therefore appeared likely that expressing *ALE1* might modify the cuticle defects observed in *zou-4* mutants, and thus diminish adhesion between the embryo and endosperm. Consistent with this, visible differences in Toluidine Blue staining were discernible between seedlings of *zou-4* and the *pSUC5::ALE1* transformed *zou-4* lines, suggesting that the cuticles of the latter were more intact than those of *zou-4* mutants (Fig. 6A-C). These results were confirmed by spectrophotometry, which showed a significant diminution in cuticle permeability associated with the presence of the *pSUC5::ALE1* transgene (Fig. 6D). Because cuticle defects have been shown to affect desiccation tolerance, and *zou-4* mutant seedlings are extremely desiccation intolerant, we devised a quantitative test for resistance to desiccation, based on the ability of 7-day-old seedlings transplanted from agar plates to survive in moderately humid conditions on soil. Conditions were selected in which 95-100% of Col0 (desiccation tolerant) and *ale1-1* seedlings, consistently survived transplantation, whereas ~50% of *zou-4* seedlings died within 3 weeks of transplantation (see Materials and methods). Using these conditions, and growing plants under homogeneous conditions (mixed trays), we compared the desiccation tolerance of *zou-4* mutants with *zou* mutants carrying the *pSUC5::ALE1* transgene. Experiments involved the transplantation of the germinated plantlets from batches of 100 seeds, and were carried out in triplicate. They showed a significant increase in desiccation tolerance, particularly in line 8, consistent with a partial complementation of the *zou-4* cuticle phenotype (Fig. 6E).

ZOU, *ALE1*, *GSO1* and *GSO2* act in the same pathway to specify embryonic cuticle formation

Double *gso1-1/gso2-1* mutants show a severe defect in embryonic cuticle development that leads to extreme permeability of cotyledon surfaces to Toluidine Blue (Tsuwamoto et al., 2008). In addition, embryos adhere to endosperm during their development, and this causes them to bend abnormally as they elongate, giving rise to a misshapen-seed phenotype similar to, but more severe than, that seen in *ale1* mutants (Fig. 7A-C). Despite their severe seed phenotypes, and consistent with the fact that the expression of *GSO1* and *GSO2* appears to be largely embryo specific during seed development, no persistent endosperm was observed in mature *gso1-1/gso2-1* mutant seeds (Fig. 7C; supplementary material Fig. S8). We did, however, note that adult *gso1-1/gso2-1* double mutants showed very subtle vegetative phenotypes, including slightly paler leaf colour, slightly retarded flowering and increased branching compared with wild-type plants, consistent with roles during post-germinative growth (data not shown).

In order to test genetically the relationship between GSO1-1/GSO2-1 function and the *ZOU/ALE1* pathway, multiple mutant combinations were generated between *gso1*, *gso2* and *zou-4*, and *ale1-4*. Cuticle permeability for single and multiple mutants was measured by quantification of Toluidine Blue uptake as described previously (Fig. 7G). As before, compared with Col0 seedlings, *ale1-4* mutant seedlings show slight, but significant increases in cuticle permeability, whereas *zou-4* mutant seedlings showed a strong increase in cuticle permeability. Consistent with previous

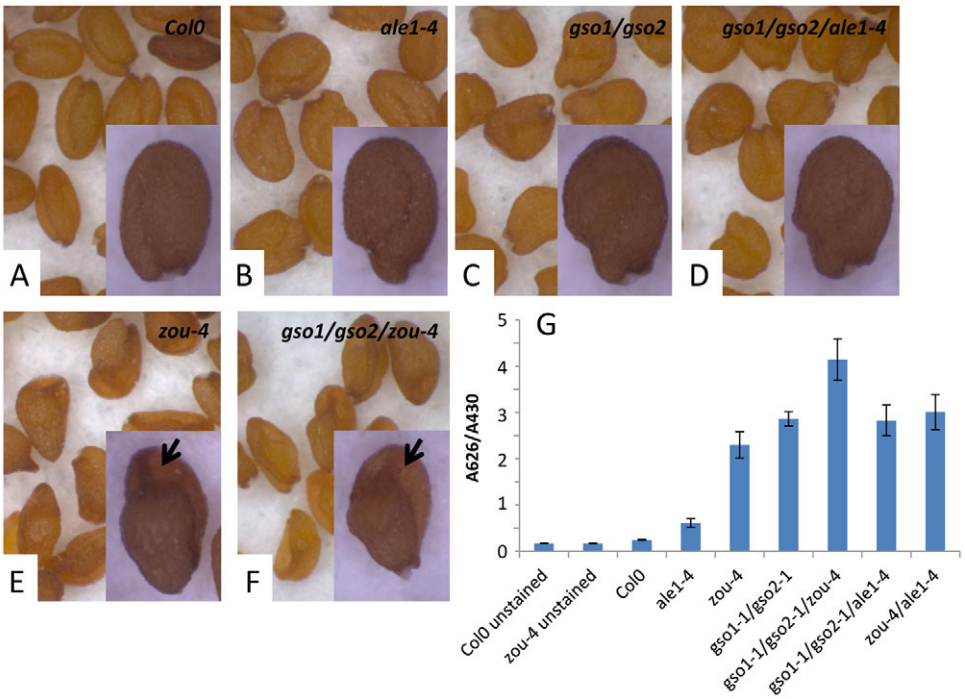

Fig. 7. GSO1 and GSO2 act in the same embryonic cuticle development pathway as ALE1 and ZOU. (**A-F**) Seed phenotypes of Col0, *ale1-4, gso1-1/gso2-1, gso1-1/gso2-1/ale1-4, zou-4* and *gso1-1/gso2-1/zou-4* homozygous mutant plants, respectively. No differences in seed phenotypes are visible between *gso1-1/gso2-1* and *gso1-1/gso2-1/ale1-4,* or between *zou-4* and *gso1-1/gso2-1/zou-4* seeds. Arrows in E and F indicate the pouch of persistent endosperm present in *zou* seeds. (**G**) Toluidine Blue uptake in seedlings from these lines was quantified spectrophotometrically, showing no significant difference in Toluidine Blue uptake between *gso1-1/gso2-1* and *gso1-1/gso2-1/ale1-4.* The difference between *gso1-1/gso2-1* and *gso1-1/gso2-1/zou-4* is largely explained by the small size of these seedlings (see supplementary material Fig. S10). Error bars represent s.d. between three biological replicates each containing 20 seedlings. Corresponding seedling phenotypes are shown in supplementary material Fig. S9.

results (Yang et al., 2008), *zou-4* showed complete epistasis with *ale1-4* using this technique and *gso1-1/gso2-1* double mutants had extremely permeable cuticles (Tsuwamoto et al., 2008). Triple *gso1-1/gso2-1/zou-4* and *gso1-1/gso2-1/ale1-4* mutants were both viable. In the case of *gso1-1/gso2-1/ale1-4* mutants, both plant phenotypes, and seed and seedling phenotypes were indistinguishable from *gso1-1/gso2-1* double mutants (Fig. 7C,D; supplementary material Fig. S9). In addition, cuticle permeability in the *gso1-1/gso2-1/ale1-4* triple mutant was indistinguishable from that in the *gso1-1/gso2-1* double mutant (Fig. 7G). In the case of *gso1-1/gso2-1/zou-4*, adult plants were indistinguishable from *gso1-1/gso2-1* double mutants and seed phenotypes were indistinguishable from those of *zou-4* single mutants (Fig. 7E,F). Thus, *GSO1* and *GSO2* show epistasis with *ALE1* with respect to embryonic cuticle formation, and probably act in the same developmental pathway. *gso1-1/gso2-1/zou-4* triple mutants seedlings were small (similar to *zou-4* mutant seedlings) (Fig. 7G; supplementary material Fig. S9). The apparent increase in cuticle permeability of *gso1-1/gso2-1/zou-4* triple mutants compared with either *zou-4* single mutants or *gso1-1/gso2-1* double mutants, is partly attributable to their small size (and thus their low chlorophyll content) (supplementary material Fig. S10), and may also reflects the additional effects of the *ALE1/GSO1/GSO2*-independent cell-death defect present in the *zou* mutants, upon embryo cuticle deposition.

DISCUSSION

In this paper, we aim to clarify a major issue regarding the mutant phenotype shown by *zou* mutants: whether cuticular defects observed in *zou* mutants are an indirect consequence of the abnormal maintenance of intact endosperm cells in the region surrounding the embryo, or whether they indicate the loss of a specific and autolysis-independent pathway via which the endosperm regulates embryonic cuticle formation. We have focused on the gene *ALE1*, which we previously shown to be strongly downregulated in *zou* mutants. Previous analyses of *ale1* mutants had shown abnormalities in embryonic cuticle formation, and adhesion to endosperm during seed development. However, they did not address directly whether *ALE1* mutants showed any defects in cell death pathways. It was therefore unclear whether ZOU acted through ALE1 (and potentially other functionally redundant proteins) to regulate both cell death and cuticle formation, or whether ALE1 was involved uniquely in embryonic cuticle formation, making the two functions of *ZOU* potentially separable.

By identifying new null alleles of *ALE1* and analysing these at the phenotypic level, we have shown that loss of *ALE1* function affects embryonic cuticle formation, and that this causes embryonic adhesion to other seed tissues and seed malformation. However, *ale1* mutants show no apparent defects in endosperm autolysis. We subsequently analysed the expression of several genes that we identified as being downregulated in *zou* mutant seeds, in *ale1* mutants. Only a subset of these genes is significantly downregulated in *ale1* mutants, further supporting our argument that the function of *ALE1* only partially overlaps with that of *ZOU*.

The ultimate proof that the two functions of *ZOU* are separable is to rescue one without affecting the other. This was achieved by re-introducing *ALE1* function into a *zou* mutant. We had previously

shown that the expression of *AtSUC5*, the spatial distribution of which closely resembles that of both *ZOU* and *ALE1*, is not affected in *zou* mutants, providing a powerful means of specifically reintroducing *ALE1* expression into *zou* mutants. In *zou* mutant plants transformed with *pSUC5:ALE1*, cuticle defects characteristically shown by *zou* mutants are significantly alleviated, whereas endosperm autolysis remains defective to the same extent as in *zou* mutants.

Although we can significantly alleviate cuticle defects in the *zou* mutant by reintroducing *ALE1* expression under *pSUC5*, we could not fully rescue this aspect of the zou phenotype. One potential reason for this is that the temporal expression pattern of *pSUC5* is not identical to that of *ALE1*, leading to lower *ALE1* expression at later developmental stages in *zou* plants expressing *pSUC5::ALE1* than in wild-type plants. However, *pSUC5::ALE1* fully complements the *ale1* mutant phenotype, suggesting that this is not a satisfactory explanation. The cuticular phenotype of null *ale1* mutants is weaker than that of *zou* mutants, and it is therefore possible that *ALE1* shows a partial functional redundancy with additional targets of ZOU that regulate embryonic cuticle formation. This possibility is currently under investigation. However, we cannot exclude a third factor, which is that persistence of the endosperm has some effect on cuticle formation. For example, persistent endosperm could physically impede the secretion of a normal cuticle even in the presence of *ALE1*.

Although our results show that ALE1 can normalize cuticle formation in the absence of endosperm autolysis, the issue still remains of how endogenous expression of *ALE1* is regulated. It is not yet clear whether *ALE1* is a direct target of ZOU, or whether its expression is regulated by other ZOU targets. We cannot formally exclude, for example, the possibility that components of the endosperm autolytic pathway are necessary for normal *ALE1* expression. However, the fact that *ALE1* expression is first detected well before the onset of autolysis makes this scenario unlikely.

ALE1 belongs to a family of secreted proteases that are widely implicated in cell signalling, and in particular in the processing of peptide ligands (Liu et al., 2009; Rautengarten et al., 2005). The fact that *ALE1* acts to regulate cuticle biosynthesis independently of endosperm autolysis strengthens the argument for the presence of a non-autonomous signalling pathway by which endosperm-specific components (such as ALE1) regulate embryonic cuticle biosynthesis. We therefore asked whether any of the four receptor kinases previously implicated in the formation of embryonic epidermis might act in the same pathway as ALE1. Genes encoding two of these kinases, *ABNORMAL LEAF SHAPE2* (*ALE2*) and *ARABIDOPSIS CRINKLY4* (*ACR4*), show synergistic genetic interactions with *ALE1* (Tanaka et al., 2007). Double mutants of either gene with *ale1* show embryo lethality owing to dramatic increases in epidermal and cuticle defects compared with single mutants (Tanaka et al., 2007; Watanabe et al., 2004). Moreover, *ale2* mutants are epistatic to *acr4* mutants, suggesting that ACR4 and ALE2 act together in a pathway parallel to that containing ALE1 (Tanaka et al., 2007). We therefore tested whether two other redundantly acting receptor kinases, GSO1 and GSO2, might act in the ALE1 pathway. The complete epistasis we observed between *gso1-1/gso2-1* double mutants and *ale1* contrasts sharply with the synergistic interaction observed between *ALE1* and *ACR4* or *ALE2*, and provides convincing evidence that GSO1 and GSO2 act in the same pathway as ALE1, reinforcing previous observations suggesting that two major pathways are involved in regulation of epidermal development during *Arabidopsis* embryogenesis (Tanaka et al., 2007). Because *GSO1* and *GSO2* are strongly expressed in embryo tissues, whereas both *ALE1* and *ZOU* show endosperm specific expression, it is tempting to speculate that the GSO receptor-kinases act redundantly to perceive a peptide ligand processed in the extra-embryonic space by ALE1 that is necessary for normal cuticle deposition on the embryonic surface. Although the identity and developmental origin of the putative ligand remain to be determined, these results represent a key indication that direct ligand-mediated signalling between the two zygotically derived seed components is necessary for normal embryonic development.

ZOU is an ancient and highly conserved transcription factor, with clear orthologues in monocotyledonous plants and even in gymnosperms and *Selaginella*. We have previously proposed that ZOU could have had an ancestral role in gymnosperms and clubmosses, permitting invasive embryo growth into maternally derived nutritive tissues. Subtilisin-like serine proteases are found in eudicot, monocot, gymnosperm, clubmoss and moss genomes. Interestingly, however, ALE1 does not have clearly defined orthologues outside the angiosperms. It is therefore possible that the function of ALE1 in regulating embryonic cuticle development was acquired during the radiation of the angiosperms. The concomitant and rapid development of the endosperm and embryo after fertilization of the angiosperm ovule may impose unique problems for both organisms, especially in terms of defining boundaries. We propose that *ALE1* may have been recruited in some angiosperms to counter such problems.

Acknowledgements
We are very grateful to Professor Y. Takahata (Laboratory of Plant Breeding, Faculty of Agriculture, Iwate University, Japan) for providing *gso1-1* and *gso2-1* mutant seeds. We acknowledge the work of the Nottingham *Arabidopsis* Stock Centre, who provided other seed lines.

Funding
This work was supported by a L'Agence Nationale de la Recherche (ANR) (France) 'Chaire D'Excellence', MECANOGRAINE, awarded to G.I. and supporting A.C. Q.X. is funded by a China Scholarship. A.W. is supported by a Biotechnology and Biological Sciences Research Council studentship. H.T. is supported by the Human Frontier Science Program (Career Development Award).

Competing interests statement
The authors declare no competing financial interests.

Supplementary material
Supplementary material available online at
http://dev.biologists.org/lookup/suppl/doi:10.1242/dev.088898/-/DC1

References

Baud, S., Wuillème, S., Lemoine, R., Kronenberger, J., Caboche, M., Lepiniec, L. and Rochat, C. (2005). The AtSUC5 sucrose transporter specifically expressed in the endosperm is involved in early seed development in Arabidopsis. *Plant J.* **43**, 824-836.

Bethke, P. C., Libourel, I. G., Aoyama, N., Chung, Y. Y., Still, D. W. and Jones, R. L. (2007). The Arabidopsis aleurone layer responds to nitric oxide, gibberellin, and abscisic acid and is sufficient and necessary for seed dormancy. *Plant Physiol.* **143**, 1173-1188.

Garcia, D., Saingery, V., Chambrier, P., Mayer, U., Jürgens, G. and Berger, F. (2003). Arabidopsis haiku mutants reveal new controls of seed size by endosperm. *Plant Physiol.* **131**, 1661-1670.

Kondou, Y., Nakazawa, M., Kawashima, M., Ichikawa, T., Yoshizumi, T., Suzuki, K., Ishikawa, A., Koshi, T., Matsui, R., Muto, S. et al. (2008). RETARDED GROWTH OF EMBRYO1, a new basic helix-loop-helix protein, expresses in endosperm to control embryo growth. *Plant Physiol.* **147**, 1924-1935.

Kurdyukov, S., Faust, A., Nawrath, C., Bär, S., Voisin, D., Efremova, N., Franke, R., Schreiber, L., Saedler, H., Métraux, J. P. et al. (2006a). The epidermis-specific extracellular BODYGUARD controls cuticle development and morphogenesis in Arabidopsis. *Plant Cell* **18**, 321-339.

Kurdyukov, S., Faust, A., Trenkamp, S., Bär, S., Franke, R., Efremova, N., Tietjen, K., Schreiber, L., Saedler, H. and Yephremov, A. (2006b). Genetic and biochemical evidence for involvement of HOTHEAD in the biosynthesis of

long-chain alpha-,omega-dicarboxylic fatty acids and formation of extracellular matrix. *Planta* **224**, 315-329.

Le, B. H., Cheng, C., Bui, A. Q., Wagmaister, J. A., Henry, K. F., Pelletier, J., Kwong, L., Belmonte, M., Kirkbride, R., Horvath, S. et al. (2010). Global analysis of gene activity during Arabidopsis seed development and identification of seed-specific transcription factors. *Proc. Natl. Acad. Sci. USA* **107**, 8063-8070.

Liu, J. X., Srivastava, R. and Howell, S. (2009). Overexpression of an Arabidopsis gene encoding a subtilase (AtSBT5.4) produces a clavata-like phenotype. *Planta* **230**, 687-697.

Lolle, S. J., Cheung, A. Y. and Sussex, I. M. (1992). Fiddlehead: an Arabidopsis mutant constitutively expressing an organ fusion program that involves interactions between epidermal cells. *Dev. Biol.* **152**, 383-392.

Penfield, S., Rylott, E. L., Gilday, A. D., Graham, S., Larson, T. R. and Graham, I. A. (2004). Reserve mobilization in the Arabidopsis endosperm fuels hypocotyl elongation in the dark, is independent of abscisic acid, and requires PHOSPHOENOLPYRUVATE CARBOXYKINASE1. *Plant Cell* **16**, 2705-2718.

Pruitt, R. E., Vielle-Calzada, J. P., Ploense, S. E., Grossniklaus, U. and Lolle, S. J. (2000). FIDDLEHEAD, a gene required to suppress epidermal cell interactions in Arabidopsis, encodes a putative lipid biosynthetic enzyme. *Proc. Natl. Acad. Sci. USA* **97**, 1311-1316.

Rautengarten, C., Steinhauser, D., Büssis, D., Stintzi, A., Schaller, A., Kopka, J. and Altmann, T. (2005). Inferring hypotheses on functional relationships of genes: Analysis of the Arabidopsis thaliana subtilase gene family. *PLoS Comput. Biol.* **1**, e40.

Stewart, C. N., Jr and Via, L. E. (1993). A rapid CTAB DNA isolation technique useful for RAPD fingerprinting and other PCR applications. *Biotechniques* **14**, 748-750.

Tanaka, H., Onouchi, H., Kondo, M., Hara-Nishimura, I., Nishimura, M., Machida, C. and Machida, Y. (2001). A subtilisin-like serine protease is required for epidermal surface formation in Arabidopsis embryos and juvenile plants. *Development* **128**, 4681-4689.

Tanaka, T., Tanaka, H., Machida, C., Watanabe, M. and Machida, Y. (2004). A new method for rapid visualization of defects in leaf cuticle reveals five intrinsic patterns of surface defects in *Arabidopsis*. *Plant Journal* **37**, 139-146.

Tanaka, H., Watanabe, M., Sasabe, M., Hiroe, T., Tanaka, T., Tsukaya, H., Ikezaki, M., Machida, C. and Machida, Y. (2007). Novel receptor-like kinase ALE2 controls shoot development by specifying epidermis in Arabidopsis. *Development* **134**, 1643-1652.

Terry, D. E., Chopra, R. K., Ovenden, J. and Anastassiades, T. P. (2000). Differential use of Alcian blue and toluidine blue dyes for the quantification and isolation of anionic glycoconjugates from cell cultures: application to proteoglycans and a high-molecular-weight glycoprotein synthesized by articular chondrocytes. *Anal. Biochem.* **285**, 211-219.

Tsuwamoto, R., Fukuoka, H. and Takahata, Y. (2008). GASSHO1 and GASSHO2 encoding a putative leucine-rich repeat transmembrane-type receptor kinase are essential for the normal development of the epidermal surface in Arabidopsis embryos. *Plant J.* **54**, 30-42.

Watanabe, M., Tanaka, H., Watanabe, D., Machida, C. and Machida, Y. (2004). The ACR4 receptor-like kinase is required for surface formation of epidermis-related tissues in Arabidopsis thaliana. *Plant J.* **39**, 298-308.

Wellesen, K., Durst, F., Pinot, F., Benveniste, I., Nettesheim, K., Wisman, E., Steiner-Lange, S., Saedler, H. and Yephremov, A. (2001). Functional analysis of the LACERATA gene of Arabidopsis provides evidence for different roles of fatty acid omega -hydroxylation in development. *Proc. Natl. Acad. Sci. USA* **98**, 9694-9699.

Yang, S., Johnston, N., Talideh, E., Mitchell, S., Jeffree, C., Goodrich, J. and Ingram, G. (2008). The endosperm-specific ZHOUPI gene of Arabidopsis thaliana regulates endosperm breakdown and embryonic epidermal development. *Development* **135**, 3501-3509.

Yephremov, A., Wisman, E., Huijser, P., Huijser, C., Wellesen, K. and Saedler, H. (1999). Characterization of the FIDDLEHEAD gene of Arabidopsis reveals a link between adhesion response and cell differentiation in the epidermis. *Plant Cell* **11**, 2187-2201.

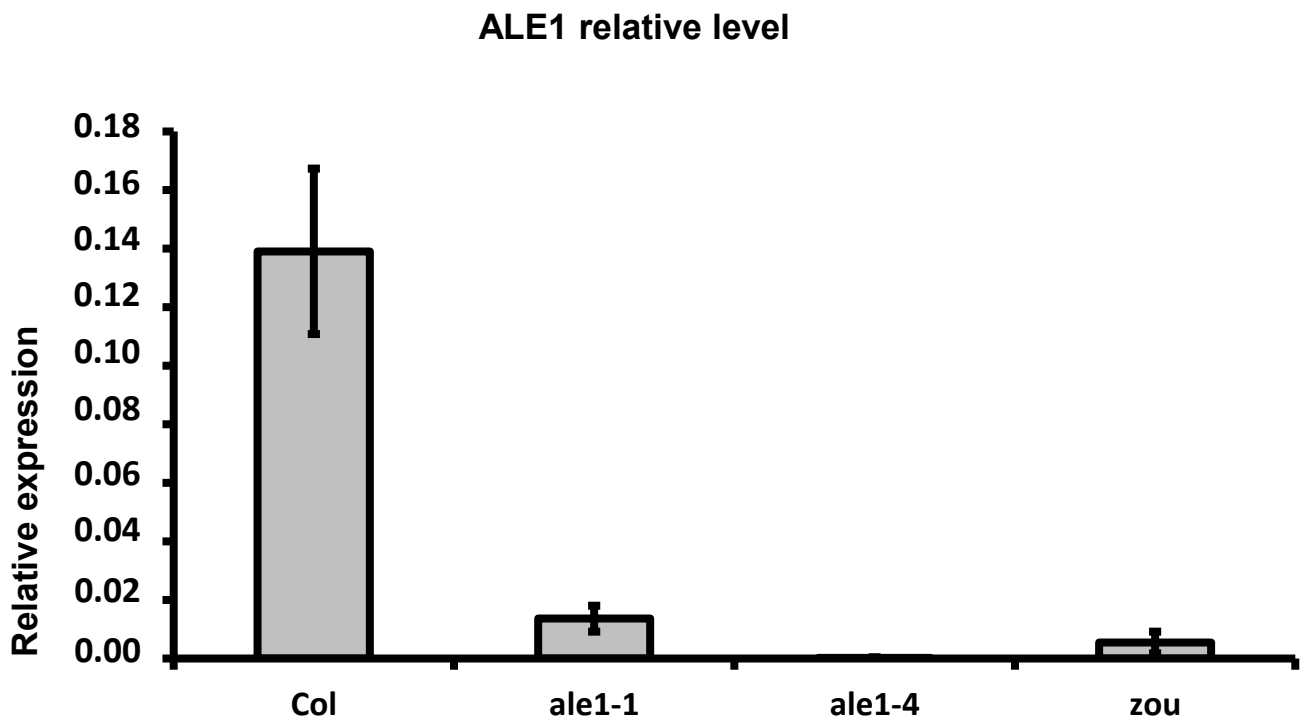

Fig. S1. Transcription *ALE1* relative to that of *EIF4* in Col0, *ale1-1, ale1-4* and *zou-4.* It should be noted that the transcripts detected in *ale1-1* may be non-functional owing to the presence of a transposon in the 3′ coding region of *ALE1* in this allele. Seed samples were taken at the late heart stage. Results are from biological triplicates, each of which was analysed in technical triplicate. Error bars represent s.d. between biological triplicates.

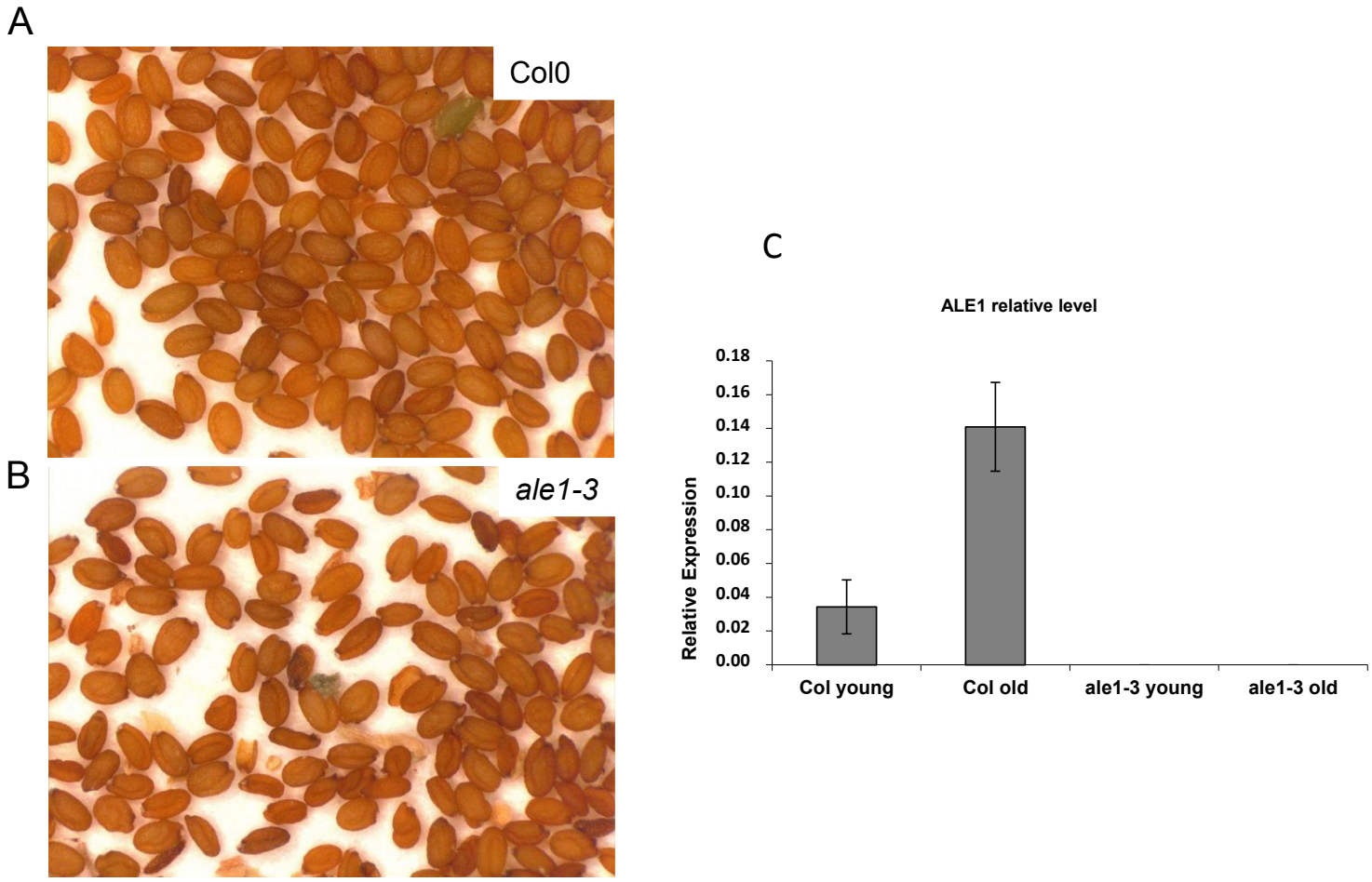

Fig. S2. Characterization of seed defects and *ALE1* expression in the *ale1-3* allele. (**A**,**B**) Seeds of wild-type (A), and concomitantly harvested *ale1-3* (B) homozygous plants. Seed-shape defects are observed in the *ale1-3* mutant. No *ALE1* transcript is detectable by Q-RT-PCR in *ale1-3* siliques either at the globular and heart stages (young), or at the torpedo stage (old). Results are from biological triplicates, each of which was analysed in technical triplicate. Error bars represent s.d. between biological triplicates.

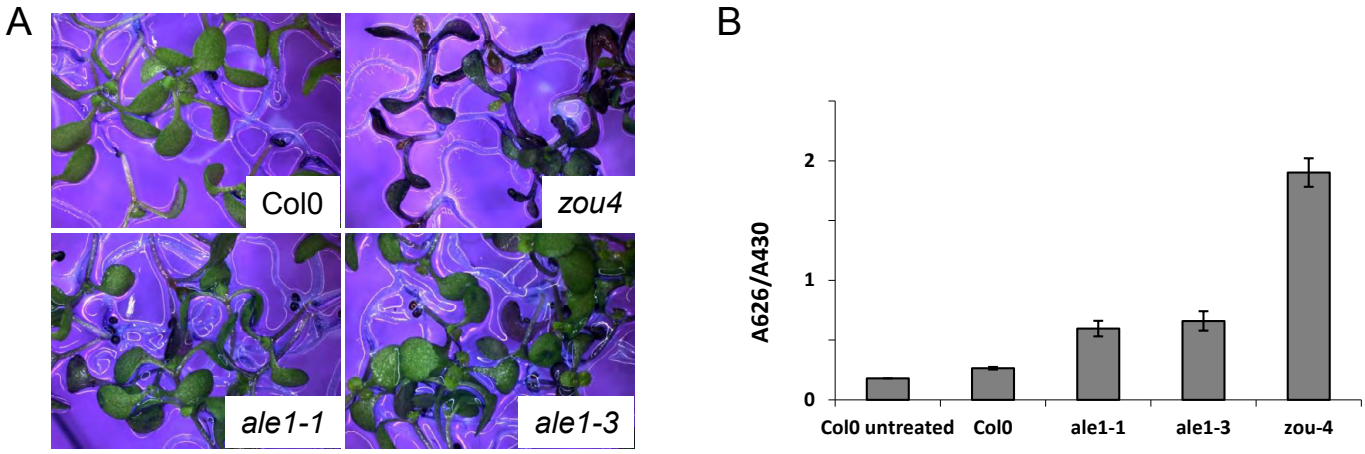

Fig. S3. Characterization of seedling cuticle defects in the *ale1-3* allele. (**A**) Toluidine Blue staining of wild-type, *ale1-1, ale1-3* and *zou-4* seedlings. (**B**) Toluidine Blue uptake in these lines was quantified spectrophotometrically, showing a significant increase in staining of *ale1-1* and *ale1-3* seedlings compared with wild type. *zou-4* seedlings stain very heavily. Error bars represent s.d. between three biological replicates each containing 20 seedlings.

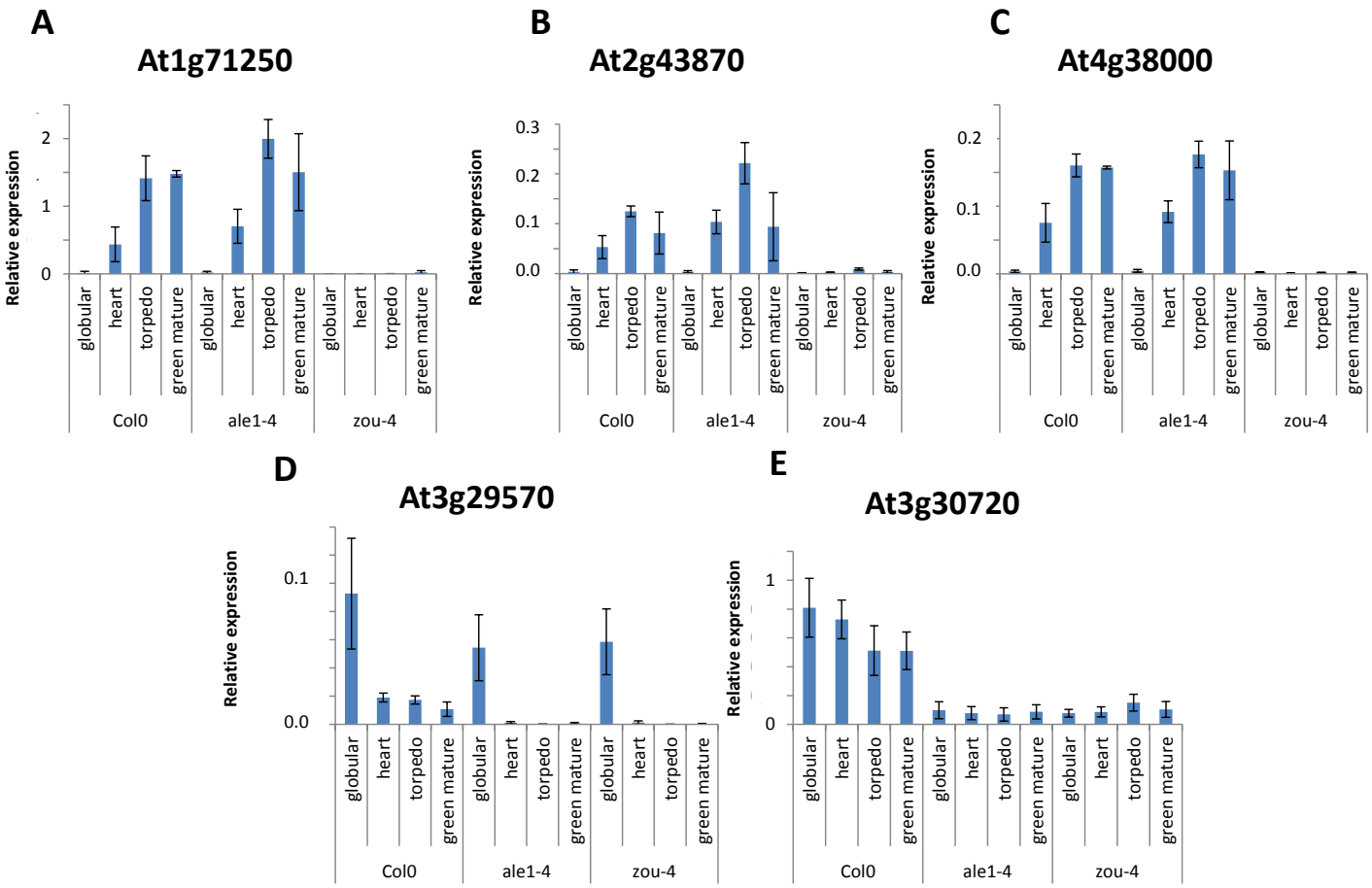

Fig. S4. ZOU and ALE1 have overlapping functions. (**A-C**) Transcription of three genes relative to that of *EIF4*, the expression of which is lost in *zou-4* mutants, but is not significantly affected in *ale1-4* mutant seeds. (**D**,**E**) Transcription of two genes relative to that of *EIF4*, the expression of which is downregulated both in *zou-4* mutants, and in *ale1-4* mutant seeds. In most cases, significant differences are seen only from the heart stage onwards. Seed samples were taken at the globular, heart, torpedo and mature green developmental stages. Results are from biological triplicates, each of which was analysed in technical triplicate. Error bars represent s.d. between biological triplicates.

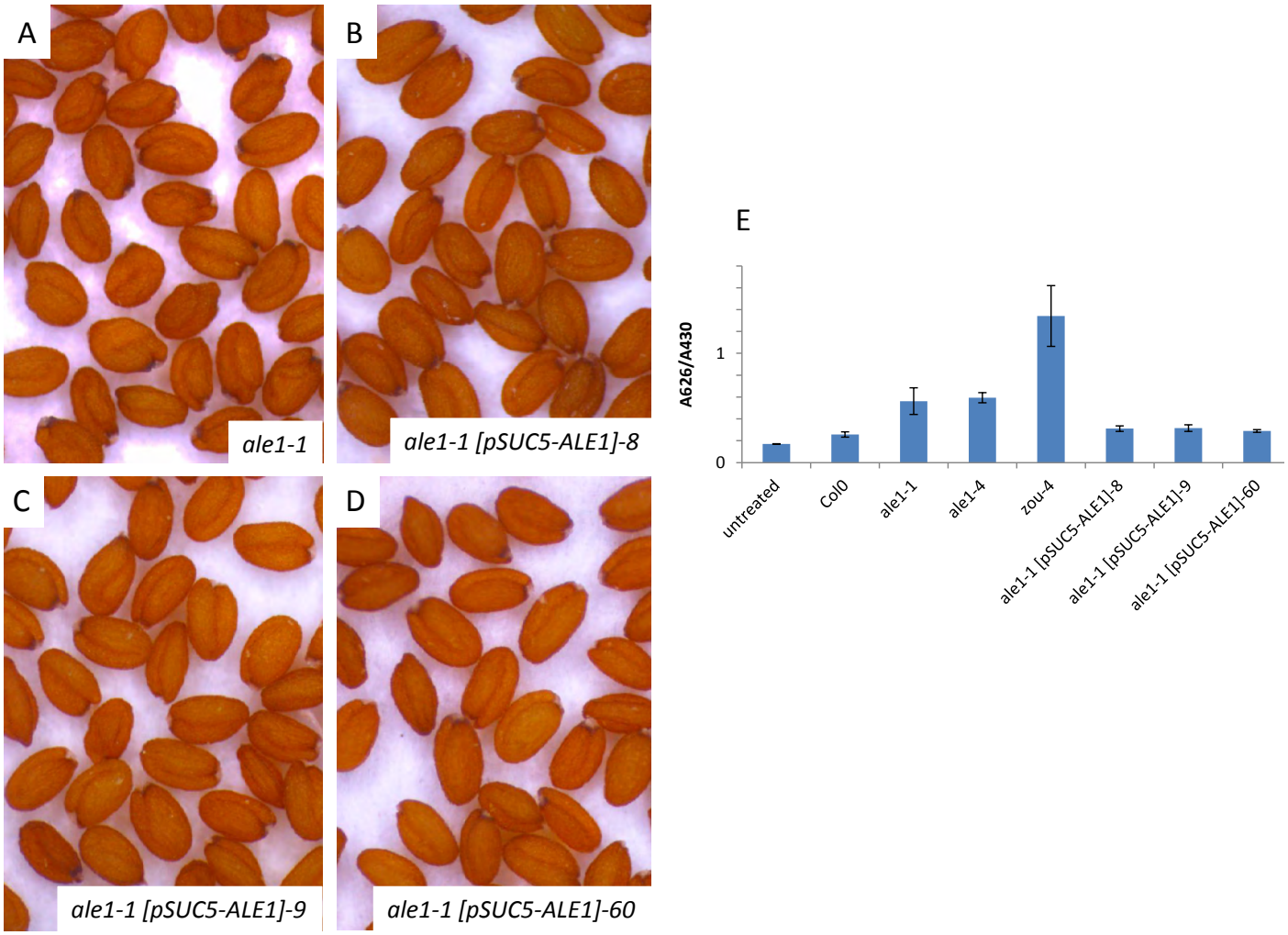

Fig. S5. Seed phenotypes. (**A-D**) *ale1-1* (A) and three independent lines of *ale1-1[pSUC5::ALE1]* (B-D), showing total rescue of the ale1 seed phenotype. (E) These same lines were subjected to Toluidine Blue staining which was quantified spectrophotometrically. The presence of the *pSUC5::ALE1* transgene rescues the cuticle phenotype of *ale1-1*. Error bars represent s.d. between three biological replicates each containing 20 seedlings.

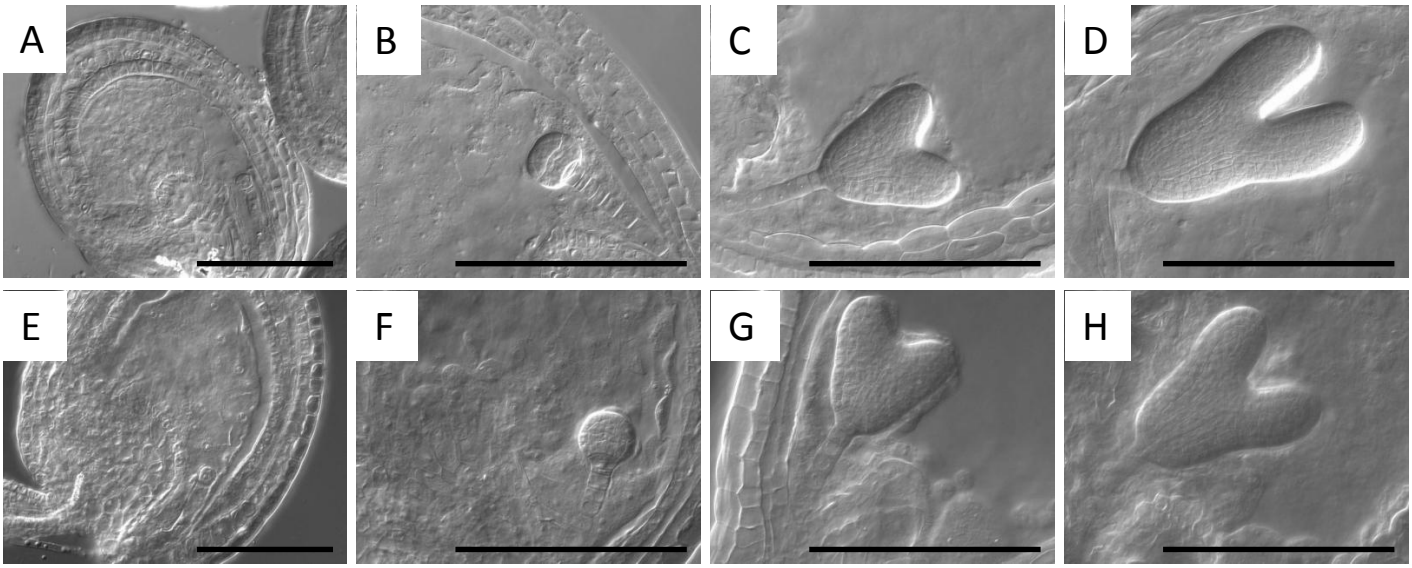

Fig. S6. Developmental staging for samples used in Fig. 5. Staging for Col0 (A-D) and *zou-4* (E-H) is shown. Developmental stages are preglobular (A,E), globular (B,F), heart (C,G) and early torpedo (D,H). Scale bar: 50 μm.

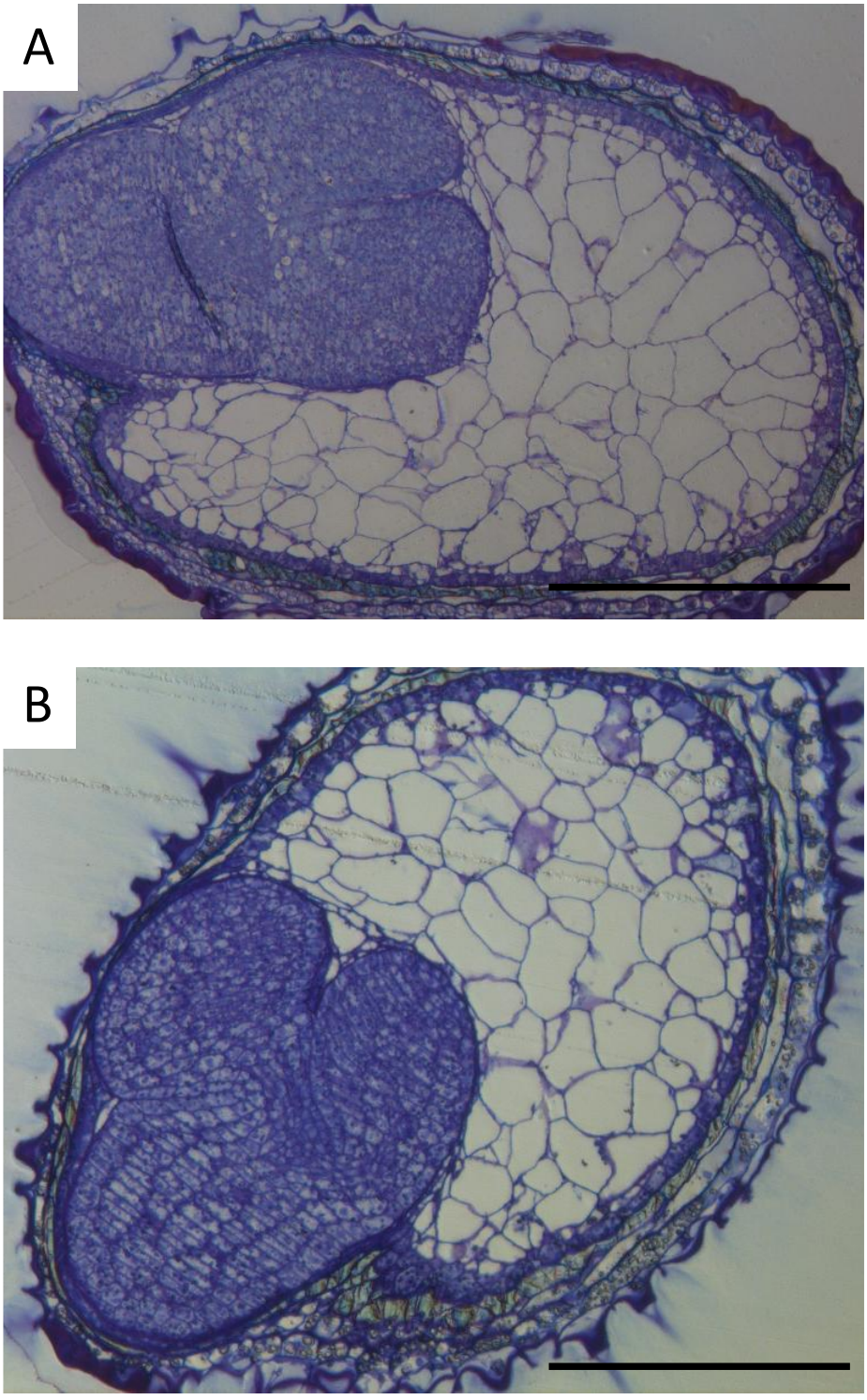

Fig. S7. Comparison of persistent endosperm phenotype. (**A**,**B**) *zou-4* (A) and *zou-4[pSUC5::ALE1]-line 8* (B). No significant loss of endosperm persistence is observed due to the introduction of the *pSUC5::ALE1* transgene. Scale bar: 100 μm

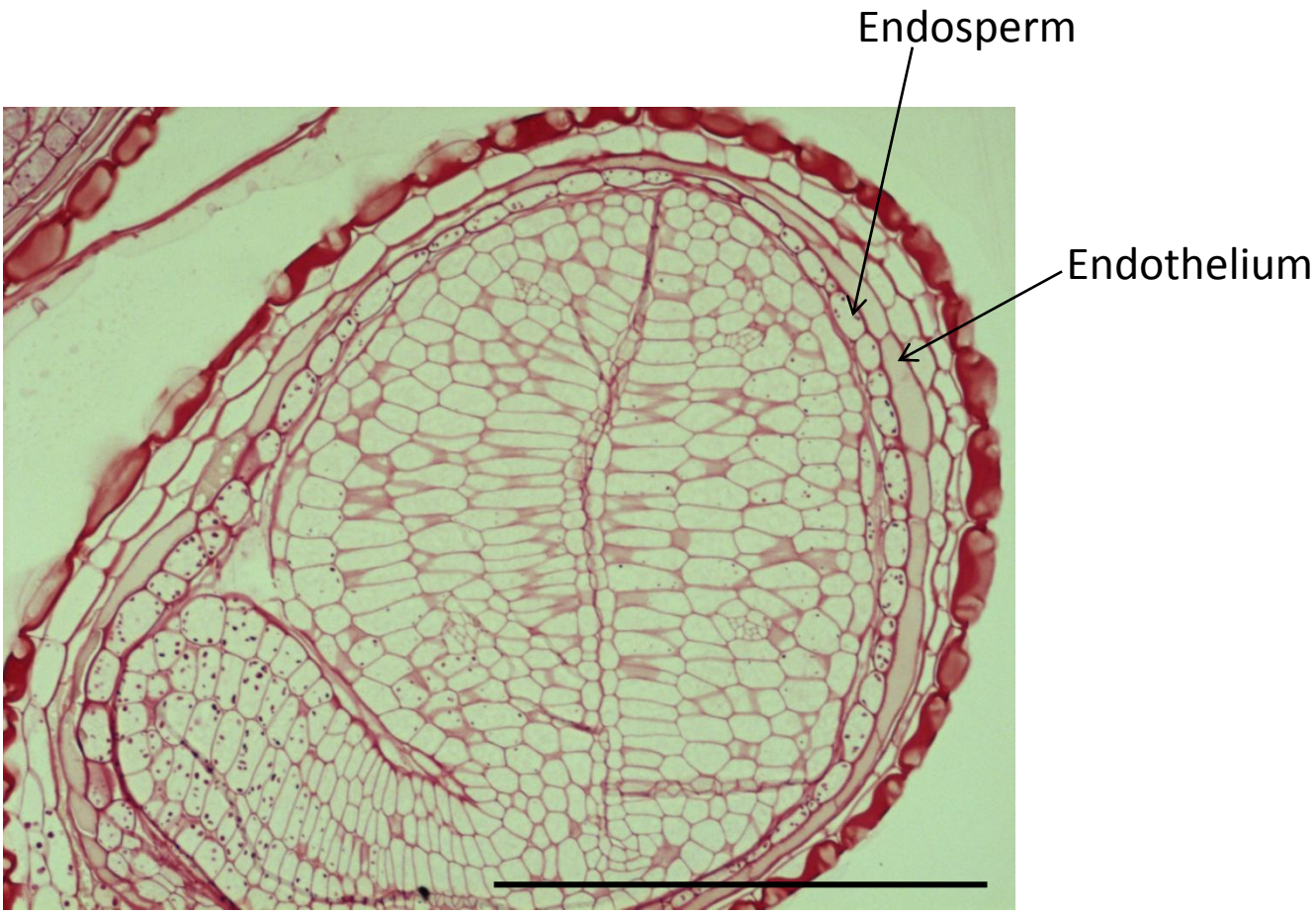

Fig. S8. *gso1-1/gso2-1* double mutant seeds do not contain a persistent endosperm. Mature, green seeds from *gso1-1/gso2-1* homozygous plants were fixed, embedded, sectioned and stained using periodic acid and Schiff's reagent (Sigma Aldrich). Only a single layer of endosperm is visible by this stage in development. Scale bar: 100 μm

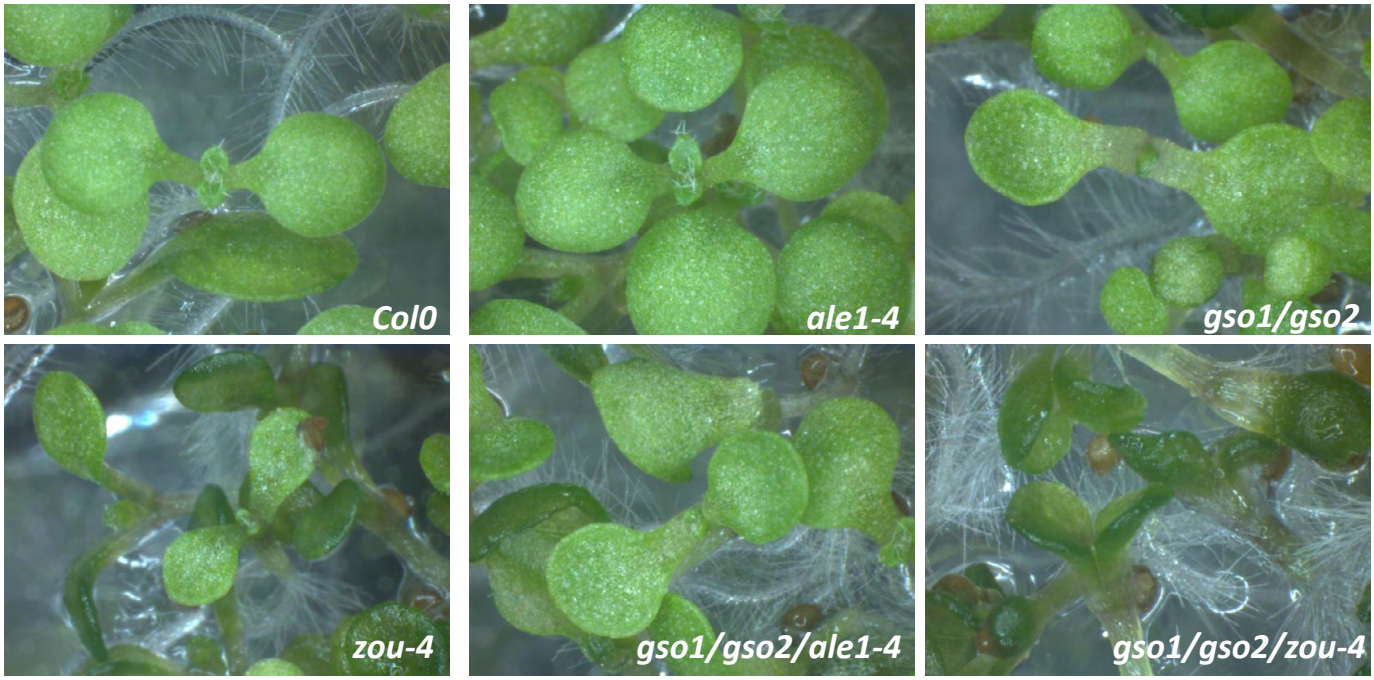

Fig. S9. Seedling phenotypes of single and multiple mutant combinations between *gso1*, *gso2*, *ale1-4* and *zou-4*. Toluidine Blue uptake in these seedlings is quantified in Fig. 7.

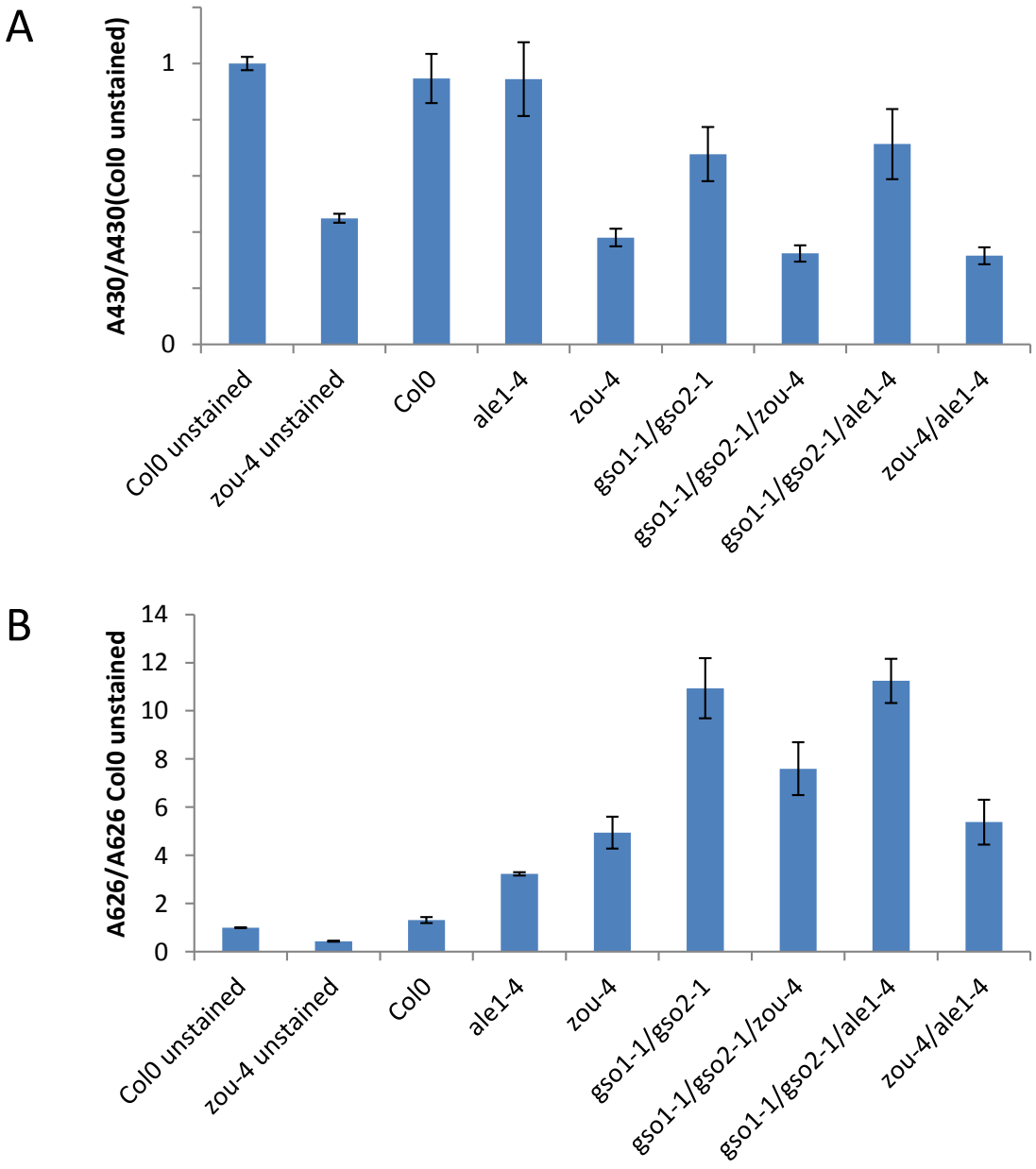

Fig. S10. Absorbance values for samples shown in Fig. 7G. Each sample contained exactly 20 seedlings and was extracted in 1 ml 80% ethanol. (**A**) A430 values (absorbance maximum for Chlorophyll A) relative to A430 for unstained Col0. The smaller size of seedlings from mutant combinations containing *zou-4* and/or *gso1-1/gso2-1* is reflected in their lower chlorophyll content. (**B**) A626 values (absorbance peak for Toluidine Blue) relative to A626 for unstained Col0.

Table S1. Primers used for Q-PCR analysis

Primer Name	Sequence
EIF4A-F (RT)	TTCGCTCTTCTCTTTGCTCTC
EIF4A-R (RT)	GAACTCATCTTGTCCCTCAAGTA
ALE1-F (RT)	AGGGCGTTGGACTATCAGG
ALE1-R (RT)	TGGCTAAGACAAGTCTGTGTTGA
At1g71250-F (RT)	TCTTAGACCTAGGCTGTAAAGAGTCA
At1g71250-R (RT)	TCAACAACTACCTTATGCCTAATCTC
At2g43870-L (RT)	aGCTTCTTTATGGGATTGTAAAAAGT
At2g43870-R (RT)	TGAGCTCTGAAATCCTATTGTCG
At4g38000-L (RT)	AAACAAGAACAAGCCTTGCAG
At4g38000-R (RT)	GATGACGTCCCGTTCGAG
At3g29570-F (RT)	TTTGCAATTTTGCATTCAGTTT
At3g29570-R (RT)	TCTGCTTCTTATTGCATCTGACTT
At3g30720-F (RT)	GGTTTGAAGCTTCTTTCAACG
At3g30720-R (RT)	TTTCTCCACAGCGACCAGTT